Available online at www.sciencedirect.com
ScienceDirect
Journal of Sound and Vibration 312 (2008) 363–379
JOURNAL OF SOUND AND VIBRATION
www.elsevier.com/locate/jsvi

# In-plane free vibration analysis of cable–arch structure

Yueyu Zhao, Houjun Kang*

*College of Mechanics and Aerospace, Hunan University, Changsha, Hunan 410082, China*

Received 20 August 2006; received in revised form 17 February 2007; accepted 15 April 2007

**Abstract**

Cable-stayed arch bridge is a new type of composite bridge, which utilizes the mechanical characters of cable and arch. Based on the supporting members of cable-stayed arch bridge and of erection of arch bridge using of the cantilever construction method with tiebacks, we propose a novel mechanical model of cable–arch structure. In this model, the equations governing vibrations of the cable–arch are derived according to Hamilton's principle for dynamic problems in elastic body under equilibrium state. Then, the program of solving the dynamic governing equations is ultimately established by the transfer matrix method for free vibration of uniform and variable cross-section, and the internal characteristics of the cable–arch are investigated. After analyzing step by step, the research results approve that the program is accurate; meanwhile, the mechanical model and method are both valuable and significant not only in theoretical research and calculation but also in design of engineering.


## 1. Introduction

The cable–arch is featured by combination flexibility of cable and stiffness of arch. For this superior structure, cable–arches are extremely efficient structural members and hence have been widely used in many long-span structures, including cable-supported roofs and cable-stayed arch bridge. Thus, the dynamic study of the cable–arches is of great engineering significance. Generally speaking, the mechanical feature results from cables and arches.

The dynamic study of the cable and arch is comparatively complicated. Due to practical importance of circular arches, many researchers have studied static as well as dynamic behavior of such elements. More than 600 articles have been summarized in review articles [1–5]. In general, the in-plane and out-of-plane vibrations of a planar arch are coupled. However, based on the Euler–Bernoulli hypothesis, if the cross-section of arch is uniform and doubly symmetric, i.e., the shear center and centroid coincide, and the in-plane and out-of-plane vibrations are uncoupled, then the out-of-plane bends and torsion responses will still be coupled.

The review shows that most of the researchers calculate the natural frequencies of arches using numerical simulations. Laura et al. [6] used the Rayleigh–Ritz method to investigate in-plane vibration of an arch with non-uniform thickness by using the classical arch theory in which the effects of axial extension, shear deformation and rotatory inertia are neglected. Chidamparam and Leissa [7] employed the Galerkin method,

*Corresponding author. Tel.: +86 731 8823962; fax: +86 731 8822722.
*E-mail address:* khjun@hnu.cn (H. Kang).

0022-460X/$ - see front matter © 2007 Published by Elsevier Ltd.
doi:10.1016/j.jsv.2007.04.038

with polynomial trial functions that satisfy the geometric boundary conditions, to obtain accurate values of free vibration frequencies. Kawakami et al. [8] derived the characteristic equation for free vibration by applying the Green function and studied the analysis for both in-plane and out-of-plane free vibration of horizontally curved beams with arbitrary shapes and variable cross-sections. In the paper of Karami and Malekzadeh [9], a differential quadrature (DQ) methodology recently developed by the authors is used to obtain a general and a computationally efficient and accurate DQ solution for free vibration of variable cross-section circular thin arches. Rubin and Tufekci [10] investigated small deformation three-dimensional free vibrations of a circular arch with uniform rectangular cross-section by using theoretical approach and finite element method. Special emphasis focused on the formulation by using the theory of the Cosserat point. Finite element results were presented and some experiments were also conducted to verify the theoretical and finite element results. Tufekci and Arpaci [11] studied the free in-plane vibrations of circular arches of uniform cross-section by considering axial extension, transverse shear and rotatory inertia effects. Recently, Tufekci and Ozzdemirci [12] and Tufekci and Dogruer [13] investigated the free in-plane and out-of-plane vibrations of a circular arch with uniform cross-section by taking into account the effects of transverse shear and rotatory inertia using the initial value method.

Similarly, the dynamic studies of the cable–arch are challenging and remain a key research field in mathematics, mechanics, and aerospace and civil engineering. It is noteworthy that the majority of the papers on this subject are restricted to the pure arches. Much less research has been focused on the cable–arches. Krishna [14] gave a review of the latest issues and developments of cable structures in tension roofs and bridges. Ju and Guo [15] investigated the in-plane elastic buckling behavior of arch and cable–arch. Cui et al. [16] and Hu and Guo [17] studied the static behavior of pre-stress cable–truss structure and the inelastic behavior of pre-stress cable–arch. However, Refs. [14–17] research on cable–arches in building constructions. Recently, Zhao et al. [18,19] presented the static and dynamic behavior of cable-stayed arch bridge as well as the differences of the internal force distribution between the bridge and the normal arch bridge. In Ref. [20], the eigenvalue buckling and nonlinear buckling of cable-stayed arch structure were investigated by establishing a two-dimensional finite element model.

In this study, the free in-plane vibration of a cable-stayed circular arch with uniform and discontinuously varying cross-section is investigated by using the transfer matrix method, but the effects of damping, axial extension, transverse shear deformation and rotary inertia are neglected. Irie et al. [21] investigated the steady-state out-of-plane response of a Timoshenko arch with internal damping in response to a sinusoidal point force or moment by using the transfer matrix method. In another work by Irie et al. [22], the transfer matrix method was adopted to study the out-of-plane free vibration of Timoshenko arches of constant radius. Hence, the transfer matrix method has been widely used for the one-dimensional acoustic analysis of engine exhaust muffler. In the present research, the transfer matrix method is employed to investigate the internal characteristics of the cable–arch and the influence of cable on the behavior of cable–arch structure. The equations, governing vibrations of the cable–arch, are derived according to Hamilton's principle for dynamic problems concerning elastic body under equilibrium state. As an approximation, cables are regarded as springs with the same stiffness and the mass is neglected. And the arch with discontinuously varying cross-sections is divided into a number of arches with constant cross-sections. For each arch element, the governing equations given in Ref. [23] are employed and the exact solution can be obtained by using the transfer matrix method. In the following, a program by using MATLAB software is presented for investigating the free vibrations of cable-stayed circular arches. The effects of numbers, stiffness, angle and position of cables and length and cross-section of arches are investigated. The investigation in this study can provide the basic guidelines to design the cable–arch structures to achieve the desired mechanical characteristics.

## 2. System and governing equations

The cable–arch structures are widely used in civil engineering. Fig. 1 shows the three kinds of cable–arch structures researched in papers [14–17]. The cable–arch (Fig. 2) is the supporting member of the cable-stayed arch bridge and of erection of arch bridge using the cantilever construction method with tiebacks. The kinematics of the cable–arch is thoroughly defined by assigning the normal displacement $v$, the tangential displacement $w$, the radius of curvature $R$, the curvilinear coordinate $s$, the angular coordinate $\varphi$, the position

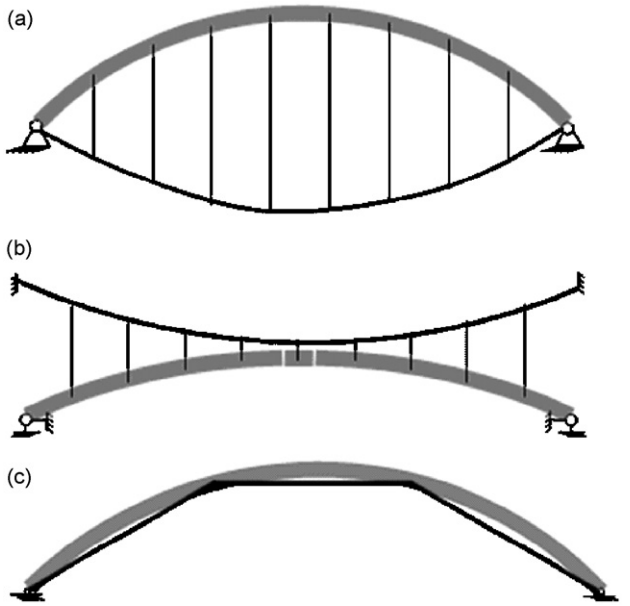


Fig. 1. Three kinds of configurations of cable–arch: (a) prestress cable–arch, (b) suspended arch and (c) cable–arch roof.

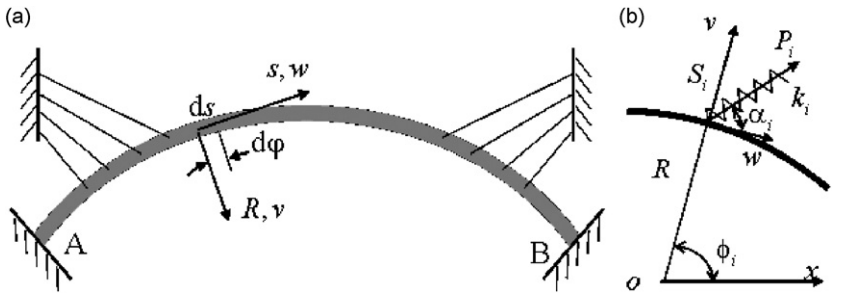


Fig. 2. Geometry and the coordinate system of cable–arch: (a) configuration of cable–arch and (b) situation of cable.

of the cables $\phi_i (i = 1, 2, \ldots, n)$ or $S_i (i = 1, 2, \ldots, n)$, and the initial tensile force of the cables $P_i (i = 1, 2, \ldots, n)$. Moreover, $\alpha_i (i = 1, 2, \ldots, n)$ denotes the angle between the cable and the tangential direction of the point $S_i$, $k_i (i = 1, 2, \ldots, n)$ denotes the axial stiffness of the cable.

The internal forces of a circular arch with uniform cross-section can be expressed by the constitutive relations [24]:

$$M = -EJ_X K_X = -EJ_X \left( \frac{\mathrm{d}^2 v}{\mathrm{d}s^2} + \frac{\mathrm{d}w}{R\mathrm{d}s} \right),$$
$$N = -EA\varepsilon = -EA \left( \frac{\mathrm{d}w}{\mathrm{d}s} - \frac{v}{R} \right), \tag{1}$$

where $M$ and $N$ denote the bending moment and the axial force, respectively. Moreover, $\varepsilon$ is the axial strain, $A$ and $J_X$ are the area and the moment of inertia of the transversal section, $E$ the Young's module and $K_X$ the curvature deflection.

The equations of motion of the cable–arch may be derived by using the Hamilton's principle. According to Hamilton's principle, the basic energy variables for the present problems required to describe the vibration behaviors of cable–arch are the strain energy $V(s, t)$, the kinetic energy $T(s, t)$ and the active energy $W(s, t)$.

The general expressions of these variables are:

$$\text{for the arch} \quad \begin{cases} V(s,t) = \dfrac{EA}{2}\int_0^S \left[\dfrac{\partial w(s,t)}{\partial s} - \dfrac{v(s,t)}{R}\right]^2 \mathrm{d}s + \dfrac{EJ_X}{2}\int_0^S \left[\dfrac{\partial^2 v(s,t)}{\partial s^2} + \dfrac{\partial w(s,t)}{R\,\partial s}\right]^2 \mathrm{d}s, \\ T(s,t) = \dfrac{\mu(s)}{2}\int_0^S \left\{\left[\dfrac{\partial w(s,t)}{\partial t}\right]^2 + \left[\dfrac{\partial v(s,t)}{\partial t}\right]^2\right\} \mathrm{d}s, \end{cases} \tag{2}$$

$$\text{for the cable} \quad \begin{cases} W(s,t) = \sum_{i=1}^{n} \delta(s - S_i)[P_i w(s,t)\cos\alpha_i + P_i v(s,t)\sin\alpha_i], \\ V(s,t) = \sum_{i=1}^{n} \delta(s - S_i)\{\frac{1}{2}k_{wi}[w(s,t)]^2 + \frac{1}{2}k_{vi}[v(s,t)]^2\}, \end{cases} \tag{3}$$

in which

$$k_{wi} = \frac{E_i A_i}{L_i}\cos\alpha_i, \quad k_{vi} = \frac{E_i A_i}{L_i}\sin\alpha_i,$$

where $E_i (i = 1, 2, \ldots, n)$ denotes the Young's modulus of the cables, $\mu(s)$ the mass per unit length of the arch, $A_i (i = 1, 2, \ldots, n)$ and $L_i (i = 1, 2, \ldots, n)$ denote the area and the length of the cable, respectively.

In general, the Hamilton's principle is expressed by the equation:

$$\delta \int_{t_1}^{t_2} [T(s,t) + W(s,t) - V(s,t)]\,\mathrm{d}t = 0. \tag{4}$$

Replacing Eqs. (2) and (3) into Eq. (4), the principle for the present problems may be expressed for an arbitrary time interval $t_1$ to $t_2$ as follows:

$$\begin{aligned} &\frac{\mu(s)}{2}\delta \int_{t_1}^{t_2}\int_0^S \left\{\left[\frac{\partial w(s,t)}{\partial t}\right]^2 + \left[\frac{\partial v(s,t)}{\partial t}\right]^2\right\} \mathrm{d}s\,\mathrm{d}t \\ &+ \delta \int_{t_1}^{t_2} \sum_{i=1}^{n} \delta(s - S_i)[P_i w(s,t)\cos\alpha_i + P_i v(s,t)\sin\alpha_i]\,\mathrm{d}t \\ &- \frac{EA}{2}\delta \int_{t_1}^{t_2}\int_0^S \left[\frac{\partial w(s,t)}{\partial s} - \frac{v(s,t)}{R}\right]^2 \mathrm{d}s\,\mathrm{d}t - \frac{EJ_X}{2}\delta \int_{t_1}^{t_2}\int_0^S \left[\frac{\partial^2 v(s,t)}{\partial s^2} + \frac{\partial w(s,t)}{R\partial s}\right]^2 \mathrm{d}s\,\mathrm{d}t \\ &- \frac{1}{2}\delta \int_{t_1}^{t_2} \sum_{i=1}^{n} \delta(s - S_i)k_{wi}[w(s,t)]^2\,\mathrm{d}t - \frac{1}{2}\delta \int_{t_1}^{t_2} \sum_{i=1}^{n} \delta(s - S_i)k_{vi}[v(s,t)]^2\,\mathrm{d}t = 0. \end{aligned} \tag{5}$$

The integrals of the variations of the individual terms of Eq. (5) have the values, on integrating by parts:

$$\begin{aligned} &\frac{\mu(s)}{2}\delta \int_{t_1}^{t_2}\int_0^S \left\{\left[\frac{\partial w(s,t)}{\partial t}\right]^2 + \left[\frac{\partial v(s,t)}{\partial t}\right]^2\right\} \mathrm{d}s\,\mathrm{d}t \\ &= \mu(s)\int_0^S \left\{\frac{\partial w(s,t)}{\partial t}\delta w(s,t)\Big|_{t_1}^{t_2} + \frac{\partial v(s,t)}{\partial t}\delta v(s,t)\Big|_{t_1}^{t_2} \right. \\ &\left. - \int_{t_1}^{t_2}\left[\frac{\partial^2 w(s,t)}{\partial t^2}\delta w(s,t) + \frac{\partial^2 v(s,t)}{\partial t^2}\delta v(s,t)\right]\mathrm{d}t\right\} \mathrm{d}s, \end{aligned} \tag{6}$$

$$\begin{aligned} &\delta \int_{t_1}^{t_2} \sum_{i=1}^{n} \delta(s - S_i)[P_i w(s,t)\cos\alpha_i + P_i v(s,t)\sin\alpha_i]\,\mathrm{d}t \\ &= \int_{t_1}^{t_2} \sum_{i=1}^{n} \delta(s - S_i)[P_i \delta w(s,t)\cos\alpha_i + P_t \delta v(s,t)\sin\alpha_i]\,\mathrm{d}t, \end{aligned} \tag{7}$$

$$\frac{EA}{2}\delta\int_{t_1}^{t_2}\int_0^S\left[\frac{\partial w(s,t)}{\partial s}-\frac{v(s,t)}{R}\right]^2\mathrm{d}s\,\mathrm{d}t=\int_{t_1}^{t_2}\left\{\left[EA\left(\frac{\partial w(s,t)}{\partial s}-\frac{v(s,t)}{R}\right)\delta w(s,t)\right]\Big|_0^L\right.$$
$$\left.-EA\int_0^S\frac{\partial}{\partial s}\left[\frac{\partial w(s,t)}{\partial s}-\frac{v(s,t)}{R}\right]\delta w(s,t)\,\mathrm{d}s-\frac{EA}{R}\int_0^S\left(\frac{\partial w(s,t)}{\partial s}-\frac{v(s,t)}{R}\right)\delta v(s,t)\,\mathrm{d}s\right\}\mathrm{d}t, \tag{8}$$

$$\frac{EJ_X}{2}\delta\int_{t_1}^{t_2}\int_0^S\left[\frac{\partial^2 v(s,t)}{\partial s^2}+\frac{\partial w(s,t)}{R\partial s}\right]^2\mathrm{d}s\,\mathrm{d}t=\int_{t_1}^{t_2}\left\{\left[EJ_X\left(\frac{\partial^2 v(s,t)}{\partial s^2}+\frac{1}{R}\frac{\partial w(s,t)}{\partial s}\right)\delta\left(\frac{\partial v(s,t)}{\partial s}\right)\right]\Big|_0^L\right.$$
$$-\left[EJ_X\frac{\partial}{\partial s}\left(\frac{\partial^2 v(s,t)}{\partial s^2}+\frac{1}{R}\frac{\partial w(s,t)}{\partial s}\right)\delta v(s,t)\right]\Big|_0^L+\frac{EJ_X}{R}\left(\frac{\partial^2 v(s,t)}{\partial s^2}+\frac{1}{R}\frac{\partial w(s,t)}{\partial s}\right)\delta w(s,t)\Big|_0^L$$
$$\left.+EJ_X\int_0^S\frac{\partial^2}{\partial s^2}\left(\frac{\partial^2 v(s,t)}{\partial s^2}+\frac{1}{R}\frac{\partial w(s,t)}{\partial s}\right)\delta v(s,t)\,\mathrm{d}s-\frac{EJ_X}{R}\int_0^S\frac{\partial}{\partial s}\left(\frac{\partial^2 v(s,t)}{\partial s^2}+\frac{1}{R}\frac{\partial w(s,t)}{\partial s}\right)\delta w(s,t)\,\mathrm{d}s\right\}\mathrm{d}t, \tag{9}$$

$$-\frac{1}{2}\delta\int_{t_1}^{t_2}\sum_{i=1}^n\delta(s-S_i)k_{wi}[w(s,t)]^2\,\mathrm{d}t-\frac{1}{2}\delta\int_{t_1}^{t_2}\sum_{i=1}^n\delta(s-S_i)k_{vi}[v(s,t)]^2\,\mathrm{d}t$$
$$=-\int_{t_1}^{t_2}\sum_{i=1}^n\delta(s-S_i)k_{wi}w(s,t)\delta w(s,t)\,\mathrm{d}t-\int_{t_1}^{t_2}\sum_{i=1}^n\delta(s-S_i)k_{vi}v(s,t)\delta v(s,t)\,\mathrm{d}t, \tag{10}$$

where

$$\delta(s-S_i)=\begin{cases}1 & s=S_i,\\ 0 & s\neq S_i.\end{cases}$$

In Eq. (6), the variations $\delta w(s,t)$ and $\delta v(s,t)$ at the instants $t_1$, $t_2$ are assumed to be zero. In Eqs. (7), (8), (9) and (10), considering the boundary conditions, one obtains:

For a hinge:

$$EJ_X\left(\frac{\partial^2 v(s,t)}{\partial s^2}+\frac{1}{R}\frac{\partial w(s,t)}{\partial s}\right)\Big|_{s=0,L}=0,\quad \delta v(s,t)\big|_{s=0,L}=0,\quad \delta w(s,t)\big|_{s=0,L}=0. \tag{11}$$

For a clamp:

$$\delta\left(\frac{\partial w(s,t)}{\partial s}\right)\Big|_{s=0,L}=0,\quad \delta\left(\frac{\partial v(s,t)}{\partial s}\right)\Big|_{s=0,L}=0,\quad \delta v(s,t)\big|_{s=0,L}=0,\quad \delta w(s,t)\big|_{s=0,L}=0. \tag{12}$$

Replacing Eqs. (6)–(10), and the boundary conditions specified in Eqs. (11) and (12), the following equations governing vibrations of the cable–arch have been derived:

$$EA\frac{\partial}{\partial s}\left(\frac{\partial w(s,t)}{\partial s}-\frac{v(s,t)}{R}\right)+\frac{EJ_X}{R}\frac{\partial}{\partial s}\left(\frac{\partial^2 v(s,t)}{\partial s^2}+\frac{1}{R}\frac{\partial w(s,t)}{\partial s}\right)-\mu(s)\frac{\partial^2 w(s,t)}{\partial t^2}$$
$$+\sum_{i=1}^n\delta(s-S_i)(P_i\cos\alpha_i-k_{wi}w(s,t))=0, \tag{13}$$

$$EJ_X\frac{\partial^2}{\partial s^2}\left(\frac{\partial^2 v(s,t)}{\partial s^2}+\frac{1}{R}\frac{\partial w(s,t)}{\partial s}\right)-\frac{EA}{R}\left(\frac{\partial w(s,t)}{\partial s}-\frac{v(s,t)}{R}\right)+\mu(s)\frac{\partial^2 v(s,t)}{\partial t^2}$$
$$+\sum_{i=1}^n\delta(s-S_i)(P_i\sin\alpha_i-k_{vi}v(s,t))=0. \tag{14}$$

Eqs. (13) and (14) derived above express a quite general vibration of cable–arch, undertaking an account of the effects of extensional axis. In practice, circular arch mostly exhibits a bending deformation, the effect of centerline compression on the deformation being negligible.

By differentiating Eq. (13) and dividing out $R$ to Eq. (14), and after appropriate manipulations, one considers the axial inextensible assumption of the circular arch

$$\varepsilon = \frac{\partial w(s,t)}{\partial s} - \frac{v(s,t)}{R} = 0$$

and

$$\mathrm{d}s = R\,\mathrm{d}\varphi.$$

The following sixth-order differential equation for the normal displacement in terms of the Hamilton's principle can be written as

$$\frac{\partial^5 v(\varphi,t)}{\partial\varphi^5} + 2\frac{\partial^3 v(\varphi,t)}{\partial\varphi^3} + \frac{\partial v(\varphi,t)}{\partial\varphi} + \frac{\mu R^4}{EJ_X}\frac{\partial^3 v(\varphi,t)}{\partial t^2\partial\varphi} + \frac{R^4}{EJ_X}\sum_{i=1}^{n}\delta(\varphi-\phi_i)\left[(k_i w(\varphi,t)+P_i)\cos\alpha_i + k_i\frac{\partial v(\varphi,t)}{\partial\varphi}\sin\alpha_i\right] = 0, \tag{15}$$

where $\varphi$ denotes the open-angle of arch.

As is evident in the equation of motion, the effects of damping, axial extension, transverse shear deformation and rotatory inertia are neglected. Although, it is assumed that the cable–arch is simply supported or clamped, Eq. (15) may be used to solve the free in-plane vibration of cable–arch whose end is free.

## 3. Free in-plane vibrations

If the kinetic energy transfer into heat is slow, disturbances may persist for some time after any forcing function is removed. There can be an important synergy between a forcing function and free vibrations of the system; such response of the system to particular forcing frequencies is most pronounced. And this phenomenon is often explored in practice by resonance testing, where the response of a structure to a localized stationary vibrating load is an important test for its safety. Thus, free vibrations of the system may have interest not only mathematically but also physically, and these occur probably in the vicinity of their original source or at significant distances away.

When $k_i = 0$ and $P_i = 0$, Eq. (15) can be expressed as linear homogeneous equation [23]:

$$\frac{\partial^5 v(\varphi,t)}{\partial\varphi^5} + 2\frac{\partial^3 v(\varphi,t)}{\partial\varphi^3} + \frac{\partial v(\varphi,t)}{\partial\varphi} + \frac{\mu R^4}{EJ_X}\frac{\partial^3 v(\varphi,t)}{\partial t^2\partial\varphi} = 0 \tag{16}$$

and has the well-known solution

$$v(\varphi,t) = V(\varphi)\sin(\omega t+\psi) \tag{17}$$

in any span $\phi_i<\varphi<\phi_{i+1}(i=1,2,\cdots,n)$, where $V(\varphi)$ is the displacement function of the system, $\omega$ the circular frequency of vibration of the system and $\psi$ the initial phase of the vibration.

Substituting Eq. (17) into Eq. (16) may yield

$$\frac{\mathrm{d}^5 V(\varphi)}{\mathrm{d}\varphi^5} + 2\frac{\mathrm{d}^3 V(\varphi)}{\mathrm{d}\varphi^3} + (1-x^2)\frac{\mathrm{d}V(\varphi)}{\mathrm{d}\varphi} = 0, \tag{18}$$

where $x$ is the circular frequency factor of the system defined by

$$x^2 = \frac{\mu\omega^2 R^4}{EJ_X}.$$

The solution can be expressed as [23]

$$V(\varphi) = C_1 + C_2\cos\alpha\varphi + C_3\sin\alpha\varphi + C_4\cos\beta\varphi + C_5\sin\beta\varphi, \tag{19}$$

where $\alpha = \sqrt{1-x}(0<x<1)$ and $\beta = \sqrt{1+x}(0<x<1)$, and

$$V(\varphi) = C_1 + C_2 \operatorname{ch}\beta\varphi + C_3 \operatorname{sh}\beta\varphi + C_4 \cos\alpha\varphi + C_5 \sin\alpha\varphi, \tag{20}$$

where $\alpha = \sqrt{x+1}(x>1)$ and $\beta = \sqrt{x-1}(x>1)$.

By using the force–displacement relations and the equilibrium conditions, the following equations has been derived:

$$w(\varphi) = C_1\varphi + \frac{C_2}{\beta}\operatorname{sh}\beta\varphi + \frac{C_3}{\beta}\operatorname{ch}\beta\varphi + \frac{C_4}{\alpha}\sin\alpha\varphi - \frac{C_5}{\alpha}\cos\alpha\varphi + C_6, \tag{21}$$

$$\theta(\varphi) = \frac{1}{R}\left[C_1\varphi + C_2\left(\frac{1}{\beta}+\beta\right)\operatorname{sh}\beta\varphi + C_3\left(\beta+\frac{1}{\beta}\right)\operatorname{ch}\beta\varphi + C_4\left(\frac{1}{\alpha}-\alpha\right)\sin\alpha\varphi + C_5\left(\alpha-\frac{1}{\alpha}\right)\cos\alpha\varphi + C_6\right], \tag{22}$$

$$M(\varphi) = -\frac{EJ_X}{R^2}\left[C_1 + C_2(1+\beta^2)\operatorname{ch}\beta\varphi + C_3(1+\beta^2)\operatorname{sh}\beta\varphi + C_4(1-\alpha^2)\cos\alpha\varphi + C_5(1-\alpha^2)\sin\alpha\varphi\right], \tag{23}$$

$$Q(\varphi) = -\frac{EJ_X}{R^3}\left[C_2(\beta^3+\beta)\operatorname{sh}\beta\varphi + C_3(\beta+\beta^3)\operatorname{ch}\beta\varphi + C_4(\alpha^3-\alpha)\sin\alpha\varphi + C_5(\alpha-\alpha^3)\cos\alpha\varphi\right], \tag{24}$$

$$N(\varphi) = \frac{EJ_X}{R^3}\left[-C_1x^2 + C_2(\beta^4+\beta^2-x^2)\operatorname{ch}\beta\varphi + C_3(\beta^4+\beta^2-x^2)\operatorname{sh}\beta\varphi + C_4(\alpha^4-\alpha^2-x^2)\cos\alpha\varphi + C_5(\alpha^4-\alpha^2-x^2)\sin\alpha\varphi\right], \tag{25}$$

where $x>1$, $C_i(i=1,2,\ldots,6)$ are the coefficients that can be represented in terms of the nodal displacements at two end nodes. Moreover, $w(\varphi)$ is the tangential displacement, $\theta(\varphi)$ the angle of rotation of the cross-section, $M(\varphi)$ the internal moment about the binormal axis, $Q(\varphi)$ the shear force of the cross-section and $N(\varphi)$ the axial force of the cross-section.

Subrahmanyam and Garg [25] developed a computer code by using a transfer matrix procedure for the solution of the beam flexure problem. Although the transfer matrix method is a traditional technique with some shortcomings, it is sometimes very convenient to use, particularly for line-like structures. The following addresses use of the transfer matrix method to study the in-plane vibration of cable–arch.

Eqs. (20)–(25) can be written in matrix form as

$$\mathbf{t} = \mathbf{T}\mathbf{c}, \tag{26}$$

in which

$$\mathbf{t} = \begin{bmatrix} w & v & \theta & M & Q & N & 1 \end{bmatrix}^{\mathrm{T}}, \quad \mathbf{c} = \begin{bmatrix} C_1 & C_2 & C_3 & C_4 & C_5 & C_6 & 1 \end{bmatrix}^{\mathrm{T}},$$

$$\mathbf{T} = \begin{bmatrix} T_{11} & T_{12} & T_{13} & T_{14} & T_{15} & T_{16} & 0 \\ T_{21} & T_{22} & T_{23} & T_{24} & T_{25} & T_{26} & 0 \\ T_{31} & T_{32} & T_{33} & T_{34} & T_{35} & T_{36} & 0 \\ T_{41} & T_{42} & T_{43} & T_{44} & T_{45} & T_{46} & 0 \\ T_{51} & T_{52} & T_{53} & T_{54} & T_{55} & T_{56} & 0 \\ T_{61} & T_{62} & T_{63} & T_{64} & T_{65} & T_{66} & 0 \\ 0 & 0 & 0 & 0 & 0 & 0 & 1 \end{bmatrix}, \tag{27}$$

where $\mathbf{t}$, $\mathbf{c}$ and $\mathbf{T}$ is the state vector of the system, the coefficient vector and the unit transfer matrix, respectively. $T_{ij}(i,j=1,2,\ldots,7)$ is written in Appendix A.

Let us consider the point $S_i(i=1,2,\ldots,n)$ that the cable is anchored on (Fig. 3), the equilibrium conditions between right cross-section and left cross-section of the point $S_i$ can be expressed by the

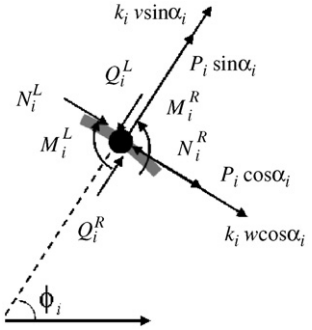


Fig. 3. Equilibrium conditions between right cross-section and left cross-section of the point $S_i$.

following formulae:

$$N_i^R = N_i^L - (P_i\cos\alpha_i + k_i w\cos\alpha_i), \quad Q_i^R = Q_i^L + (P_i\sin\alpha_i + k_i v\sin\alpha_i),$$
$$M_i^R = M_i^L, \quad \theta_i^R = \theta_i^L, \quad w_i^R = w_i^L, \quad v_i^R = v_i^L, \tag{28}$$

where the superscript $R$ and $L$ denote the right and left cross-section of the node $S_i (i = 1, 2, \ldots, n)$, respectively. Eq. (28) can be written also in matrix form as

$$\mathbf{t}_i^R = \mathbf{T}_i^N \mathbf{t}_i^L, \tag{29}$$

in which

$$\mathbf{t}_i^R = \begin{bmatrix} w_i^R & v_i^R & \theta_i^R & M_i^R & Q_i^R & N_i^R & 1 \end{bmatrix}^{\mathrm{T}}, \quad \mathbf{t}_i^L = \begin{bmatrix} w_i^L & v_i^L & \theta_i^L & M_i^L & Q_i^L & N_i^L & 1 \end{bmatrix}^{\mathrm{T}},$$

$$\mathbf{T}_i^N = \begin{bmatrix} 1 & 0 & 0 & 0 & 0 & 0 & 0 \\ 0 & 1 & 0 & 0 & 0 & 0 & 0 \\ 0 & 0 & 1 & 0 & 0 & 0 & 0 \\ 0 & 0 & 0 & 1 & 0 & 0 & 0 \\ 0 & k_i\sin\alpha_i & 0 & 0 & 1 & 0 & P_i\sin\alpha_i \\ -k_i\cos\alpha_i & 0 & 0 & 0 & 0 & 1 & -P_i\cos\alpha_i \\ 0 & 0 & 0 & 0 & 0 & 0 & 1 \end{bmatrix},$$

where $\mathbf{t}_i^R$ and $\mathbf{t}_i^L$ are the right and left state variables of the node $S_i$, and $\mathbf{T}_i^N$ is the transfer matrix of node.

One defines the initial state vector

$$\mathbf{t}_0 = \begin{bmatrix} w_0 & v_0 & \theta_0 & M_0 & Q_0 & N_0 & 1 \end{bmatrix}^{\mathrm{T}},$$

then the coefficient vector $\mathbf{c}$ in Eq. (26) can be expressed by substituting $\mathbf{t}_0$ and $\varphi = 0$ into Eq. (26) as

$$\mathbf{c} = \mathbf{T}_0^{-1}\mathbf{t}_0, \tag{30}$$

where the superscript $-1$ denotes the inverse matrix of $\mathbf{T}$ when $\varphi = 0$, and the elements of $\mathbf{T}_0^{-1}$ are written in Appendix B.

Thus, the left state vector $\mathbf{t}_1^L$ of the first point $S_1$ that the cable is anchored on is taken to be

$$\mathbf{t}_1^L = \mathbf{T}_1\mathbf{T}_0^{-1}\mathbf{t}_0, \tag{31}$$

where $\varphi = \varphi_1$ in the matrix $\mathbf{T}_1$. Considering Eq. (29) gives

$$\mathbf{t}_1^R = \mathbf{T}_1^R \mathbf{t}_0, \tag{32}$$

where $\mathbf{T}_1^R = \mathbf{T}_1^N \mathbf{T}_1 \mathbf{T}_0^{-1}$.

Similarly, $\mathbf{t}_2^R$ can be written as

$$\mathbf{t}_2^R = \mathbf{T}_2^R \mathbf{t}_1^R, \tag{33}$$

where $\mathbf{T}_2^R = \mathbf{T}_2^N \mathbf{T}_2 \mathbf{T}_0^{-1}$. Applying the transfer matrix principle, $\mathbf{t}_n^R$ can be derived

$$\mathbf{t}_n^R = \mathbf{T}_n^R \mathbf{t}_{n-1}^R = \mathbf{T}_n^R \mathbf{T}_{n-1}^R \mathbf{t}_{n-2}^R = \cdots = \mathbf{T}_n^R \mathbf{T}_{n-1}^R \mathbf{T}_{n-2}^R \cdots \mathbf{T}_1^R \mathbf{t}_0 = \mathbf{T}^R \mathbf{t}_0 \tag{34}$$

in which $\mathbf{T}^R$ is the global transfer matrix of the system and can also be written as

$$\mathbf{T}^R = \mathbf{T}_n^N \mathbf{T}_n \mathbf{T}_0^{-1} \mathbf{T}_{n-1}^N \mathbf{T}_{n-1} \mathbf{T}_0^{-1} \mathbf{T}_{n-2}^N \mathbf{T}_{n-2} \mathbf{T}_0^{-1} \cdots \mathbf{T}_2^N \mathbf{T}_2 \mathbf{T}_0^{-1} \mathbf{T}_1^N \mathbf{T}_1 \mathbf{T}_0^{-1}. \tag{35}$$

Deriving the global transfer matrix $\mathbf{T}^R(x<1)$ is analogous and the process of it is neglected. In Eq. (34), $\mathbf{T}^R$ is a $7 \times 7$ matrix, $\mathbf{t}_0$ and $\mathbf{t}_n^R$ denote the state vector at the end points A and B. Since the effect of the concentrated force $P_i$ on the natural frequencies is negligible, the system can be reduced to a homogeneous system by making $P_i = 0 (i = 1, 2, \ldots, n)$.

The boundary conditions for end point A as shown in Fig. 2 can be given:

$$\begin{aligned}
&\text{Hinged end :} \quad w(\varphi_A) = 0;\ v(\varphi_A) = 0;\ M(\varphi_A) = 0.\\
&\text{Clamped end :} \quad w(\varphi_A) = 0;\ v(\varphi_A) = 0;\ \theta(\varphi_A) = 0.\\
&\text{Free end :} \quad M(\varphi_A) = 0;\ Q(\varphi_A) = 0;\ N(\varphi_A) = 0.
\end{aligned}$$

Similar boundary conditions are specified for the end B in Fig. 2. For a nontrivial solution, the determinant of the homogeneous system must be equal to zero and this requirement will give the natural frequencies of the system (cable–arch structure) in accordance with the boundary conditions. Mode shapes are specified by substituting the factor $x$ of the circular frequency into Eq. (34). This solution procedure can also be applied to the case in which the cross-section is stepped by making the matrix $\mathbf{T}_i^N$ to be a unit matrix.

## 4. Numerical evaluations and comparisons

The dimensionless circular frequency factors $x_i = \omega_i R^2 \sqrt{\mu / EJ_x}$ are calculated for four different cases:

*Case* 1: The program of solving circular frequency factors $x_i$ is verified by finite element method.

*Case* 2: Effects of the character of cable on the circular frequency factors are considered.

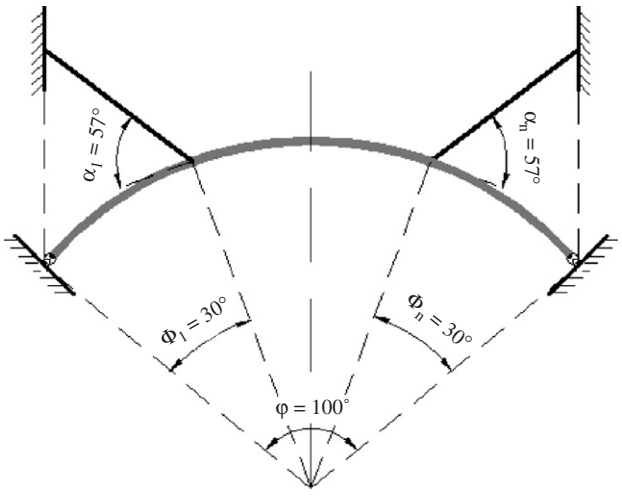


Fig. 4. Elevation of cable–arch.

*Case* 3: Effects of the parameter of the arch on the circular frequency factors are investigated.

*Case* 4: Effects of the construction process of the arch on the circular frequency factors are investigated.

The examples (Fig. 4) are solved for clamped–clamped, hinged–hinged, clamped–hinged and clamped-free end conditions. The frequency factors are calculated for the lowest five modes of vibration of the system with the following properties: the material of arch is steel with an opening angle $\varphi = 100^\circ$, Young's modulus $E_g = 2.06 \times 10^{11}$ Pa, the area of cross-section $b \times h = 0.3 \times 0.8\,\mathrm{m}^2$, the mass of unit length $\mu = 1872\,\mathrm{kg/m}$, $R = 60\,\mathrm{m}$, the material of cable is a high-strength steel wire with $A_s = 0.00255\,\mathrm{m}^2$, $E_s = 2.1 \times 10^{11}$ Pa and $P = 656.25\,\mathrm{kN}$; the other properties of the cable and arch are shown in Fig. 4.

The developed analysis was numerically implemented through a MATLAB program, which was tested for efficiency and reliability. The lowest five frequencies and periods of pure arch and cable–arch with hinged–hinged conditions are showed in Table 1 when $R = 60\,\mathrm{m}$ and $\varphi = 100^\circ$. The results of this study for frequency differ mostly by only 8% from the finite elemental solution. This comparatively favorable comparison paved the way to an analysis of the dynamic characters of cable–arch. Furthermore, it is worth noting that the frequencies of cable–arch are bigger than that of pure arch in Table 1. In other words, the cable makes the stiffness of the cable–arch bigger than pure arch in a plane. In Fig. 5, the lowest five mode shapes are given for hinged–hinged pure arch and cable–arch. There are nearly no differences between pure arch and cable–arch on the lowest five mode shapes, because the stiffness of cable is not enough to change the mode shape of pure arch.

In Fig. 6, the lowest five frequency factors are given for hinged–hinged, clamped–clamped and clamped–hinged cable–arch. The differences among the results of the various positions $\phi_i$ are considerably large, and it is obvious that the frequencies increases further with an increase in the angle $\phi_1$ when $\alpha_1 = 53^\circ$. However, the dissimilarity between the different boundary conditions: hinged–hinged, clamped–clamped and clamped–hinged is significantly small.

In Fig. 7, effects of stiffness of cable on the lowest five frequency factors are given for hinged–hinged, clamped–clamped and clamped–hinged cable–arch. Effects of numbers of cable on the lowest five frequency factors for hinged–hinged, clamped–clamped and clamped–hinged cable–arch are shown in Fig. 8. A sharp increase in the lowest five frequency factors, which is due to the increase in the stiffness and the number of cables, can be seen in Figs. 7 and 8. It shows that the in-plane stiffness of cable–arch increases while the stiffness and numbers of the cable increase. However, the effects of the boundary conditions on the frequency factors are comparatively lesser.

In Fig. 9, effects of the angle $\alpha_1$ of cable on the lowest five frequencies are given for hinged–hinged, clamped–clamped and clamped–hinged cable–arch with the situation angle $\phi_1 = 10^\circ$. It can be seen easily in the figure that the angle $\alpha_1$, due to the in-plane vibration of cable–arch, has a negligible effect.

Effects of the radius $R$ of the arch on the lowest five frequencies are shown for hinged–hinged, clamped–clamped and clamped–hinged cable–arch with the opening angle $\varphi = 100^\circ$ in Fig. 10. It is concluded from Fig. 10 that the influence of the radius $R$ on the frequency factors is important and the sharp decrease of the frequency factors is due to the increase of the radius $R$.

Table 1
Frequency and period of pure arch and cable–arch

| Mode no. | Frequency (Hz) | | | | Period (s) | | | |
|---|---|---|---|---|---|---|---|---|
| | Arch | | Cable-stayed arch | | Arch | | Cable-stayed arch | |
| | ROFEM | ROTS | ROFEM | ROTS | ROFEM | ROTS | ROFEM | ROTS |
| 1st | 0.5654 | 0.6275 | 1.4310 | 1.3328 | 1.7687 | 1.5936 | 0.6988 | 0.7503 |
| 2nd | 1.3590 | 1.4017 | 2.6260 | 2.8438 | 0.7358 | 0.7134 | 0.3808 | 0.3516 |
| 3rd | 2.5980 | 2.6675 | 4.6740 | 4.6751 | 0.3849 | 0.3749 | 0.2139 | 0.2139 |
| 4th | 4.0710 | 4.1245 | 5.5510 | 5.5732 | 0.2456 | 0.2425 | 0.1801 | 0.1794 |
| 5th | 5.9920 | 5.9920 | 7.2120 | 7.2704 | 0.1669 | 0.1669 | 0.1387 | 0.1375 |

*Note*: ROFEM = results of finite element method, ROTS = results of this study.

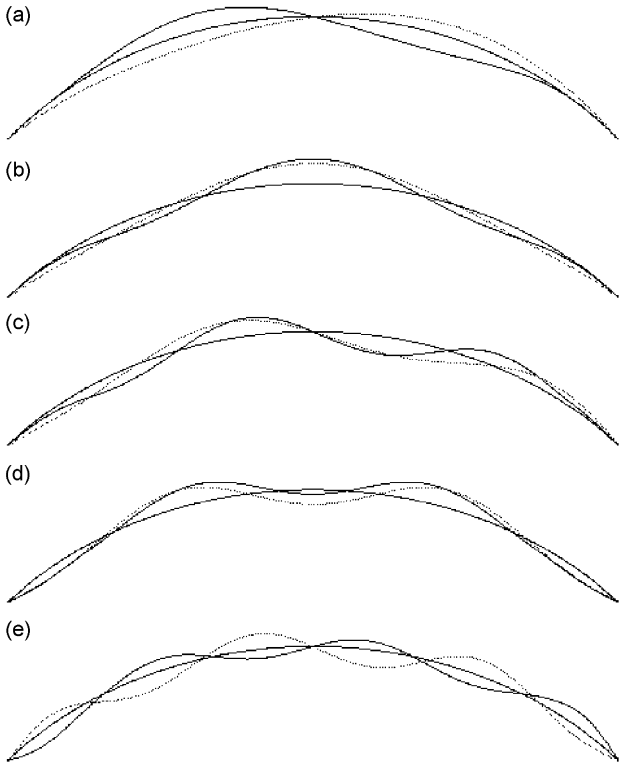


Fig. 5. The lowest five mode shapes of pure arch and cable–arch: (a) first mode, (b) second mode, (c) third mode, (d) fourth mode and (e) fifth mode. —, configuration of arch; -----, mode shape of pure arch; —, mode shape of cable–arch.

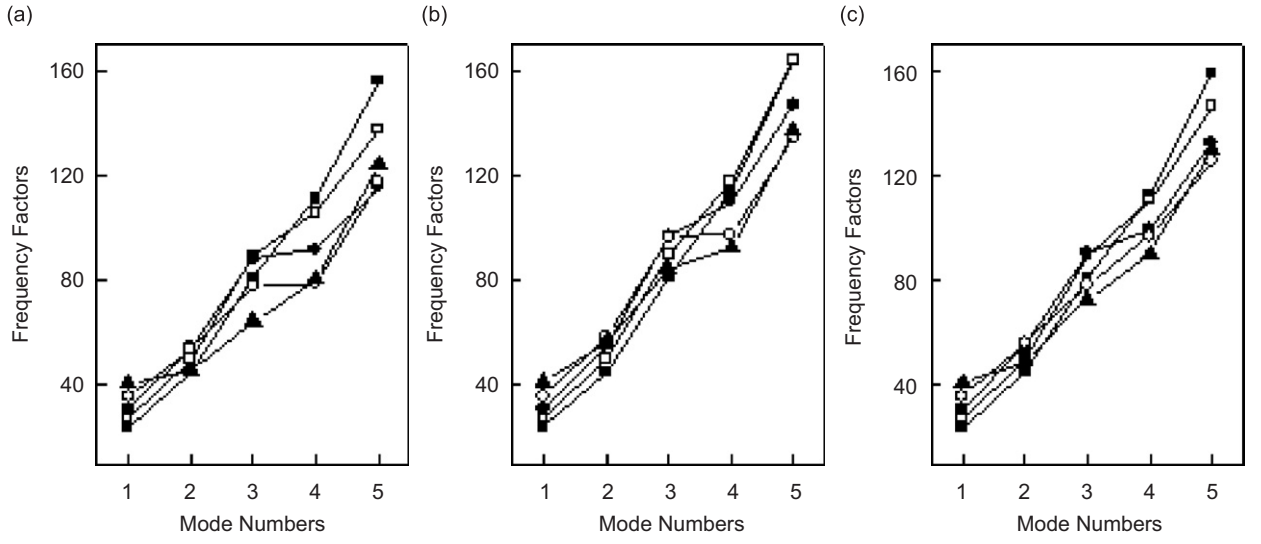


Fig. 6. Effects of situation of cable on the lowest five frequencies: (a) hinged–hinged. (b) clamped–clamped and(c) clamped–hinged. –■–, 10°; –□–, 13°; –●–, 16°; –○–, 19°; –▲–, 22°.

In Table 2, the frequencies of cable–arch of uniform and variable cross-section are given for clamped–clamped arch and cable–arch. There are two kinds of step arches. The calculations of the 'active' dimensions of the nine-step arch in this example are $h_1 = 1.1\,\text{m}$, $h_2 = 1.0\,\text{m}$, $h_3 = 0.8\,\text{m}$, $h_4 = 0.6\,\text{m}$, $h_5 = 0.5\,\text{m}$,

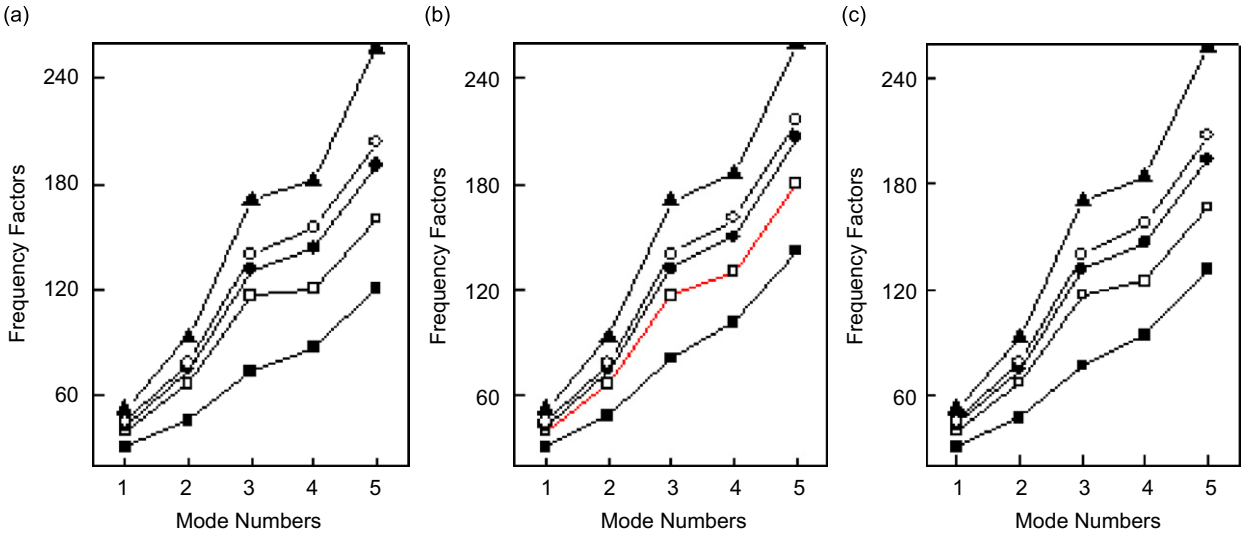


Fig. 7. Effects of stiffness of cable on the lowest five frequencies: (a) hinged–hinged, (b) clamped–clamped and (c) clamped–hinged. –■–, 0.1$A$; –□–, 0.5$A$; –●–, $A$; –○–, 1.5$A$; –▲–, 10$A$; $A$ = area of cross-section of cable.

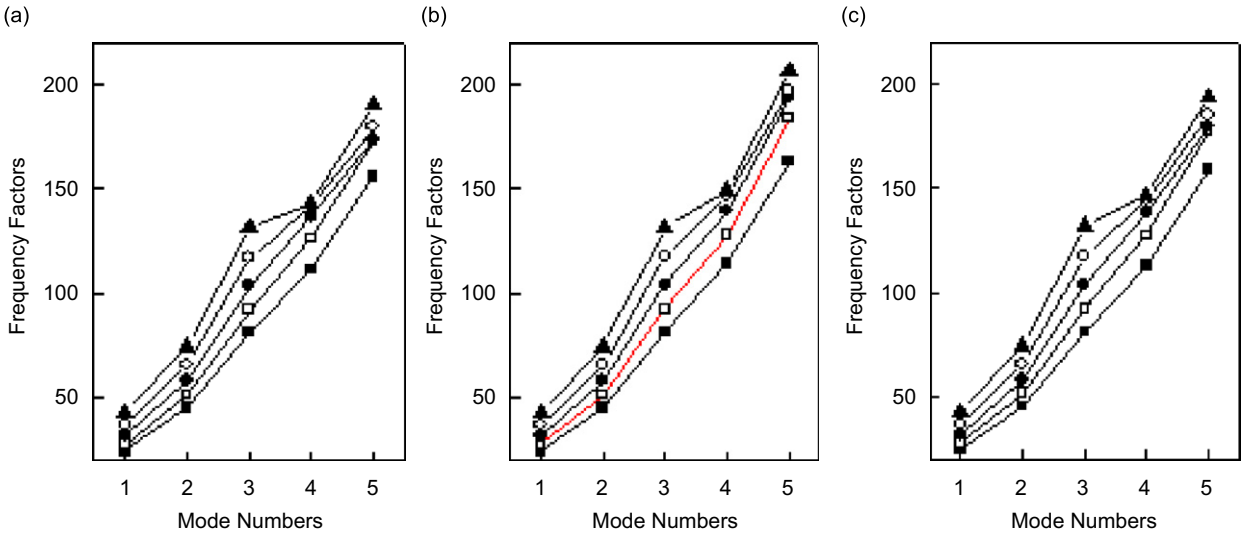


Fig. 8. Effects of numbers of cable on the lowest five frequencies: (a) hinged–hinged. (b) clamped–clamped and (c) clamped–hinged. –■–, two cables; –□–, four cables; –●–, six cables; –○–, eight cables; –▲–, ten cables.

$h_6 = 0.6\,\text{m}$, $h_7 = 0.8\,\text{m}$, $h_8 = 1.0\,\text{m}$ and $h_9 = 1.1\,\text{m}$. It is shown that the area of cross-section of the foot is bigger than that of crown (VCS1). On the contrary, the other kind step arch is VCS2, and the 'active' dimensions of the nine-step arch are $h_1 = 0.5\,\text{m}$, $h_2 = 0.6\,\text{m}$, $h_3 = 0.8\,\text{m}$, $h_4 = 1\,\text{m}$, $h_5 = 1.1\,\text{m}$, $h_6 = 1\,\text{m}$, $h_7 = 0.8\,\text{m}$, $h_8 = 0.6\,\text{m}$, $h_9 = 0.5\,\text{m}$. The height of the uniform cross-section is $h = 0.8\,\text{m}$. In Table 2, the lowest five natural frequencies of cable–arch with three kinds of cross-sections are compared: it is shown that the difference between the frequencies is considerably big and the frequencies of the cable–arch with VCS2 are the biggest. Similarly, it is also concluded from the frequencies of the pure arch.

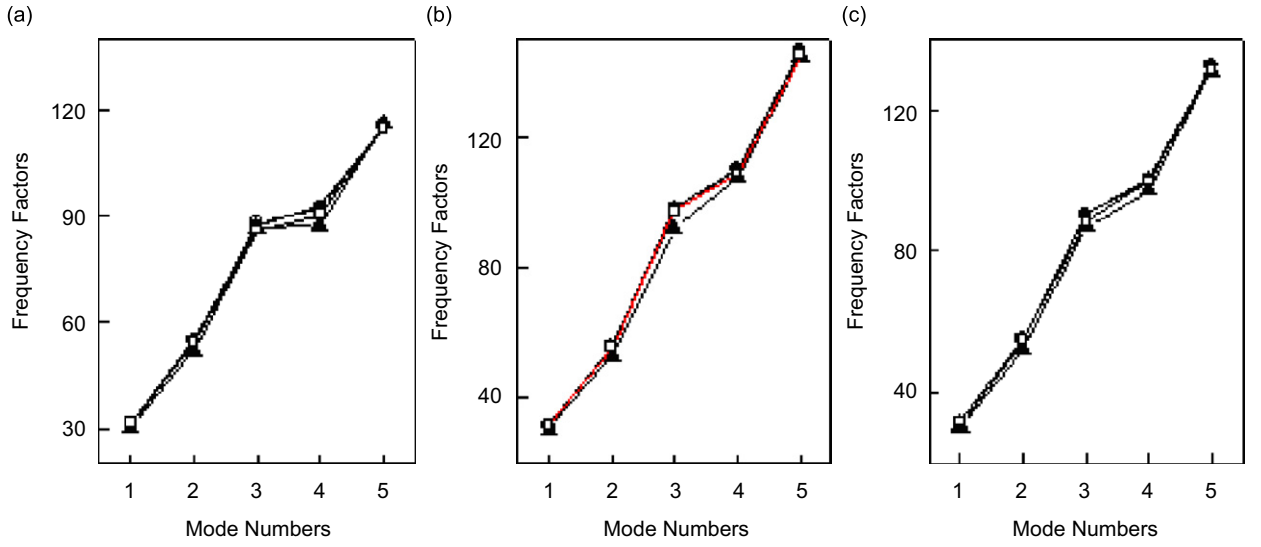


Fig. 9. Effects of the angle of cable on the lowest five frequencies: (a) hinged–hinged, (b) clamped–clamped and (c) clamped–hinged. –■–, 81.635°; –□–, 68.756°; –●–, 57.769°; –○–, 48.905°.

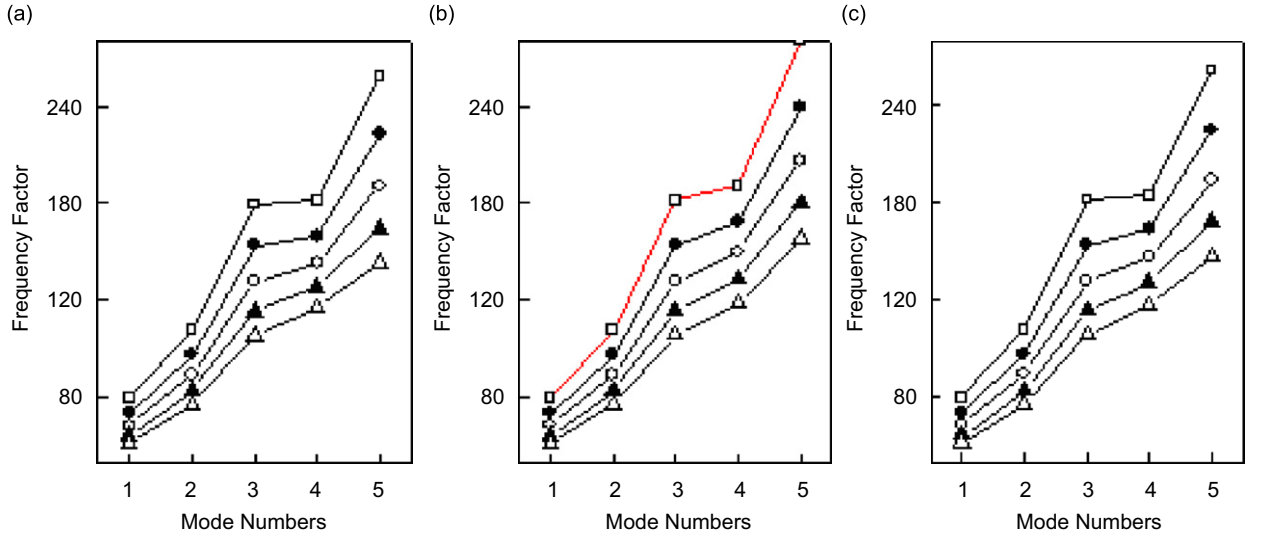


Fig. 10. Effects of the radius of arch on the lowest five frequencies: (a) hinged–hinged, (b) clamped–clamped and (c) clamped–hinged. –■–, 50 m; –□–, 55 m; –●–, 60 m; –○–, 65 m; –▲–, 70 m.

Table 2
The frequencies of cable–arch of uniform and variable cross-section (Hz)

| Mode no. | Uniform cross-section | | Variable cross-section (1) | | Variable cross-section (2) | |
|---|---|---|---|---|---|---|
| | Pure arch | Cable–arch | Pure arch | Cable–arch | Pure arch | Cable–arch |
| 1 | 0.7392 | 2.2369 | 0.6394 | 1.9887 | 0.7592 | 2.6133 |
| 2 | 1.5826 | 3.8922 | 1.5719 | 3.4258 | 1.6665 | 5.0190 |
| 3 | 2.9345 | 6.9100 | 2.8703 | 5.7491 | 2.9256 | 7.4100 |
| 4 | 4.4586 | 7.6767 | 4.2987 | 7.4772 | 4.4037 | 8.3904 |
| 5 | 6.4928 | 10.168 | 6.3738 | 9.8268 | 6.3406 | 10.393 |

*Note*: Variable cross-section (1) = the area of cross-section of the foot is bigger than that of crown; variable cross-section (2) = the area of cross-section of the foot is smaller than that of crown.

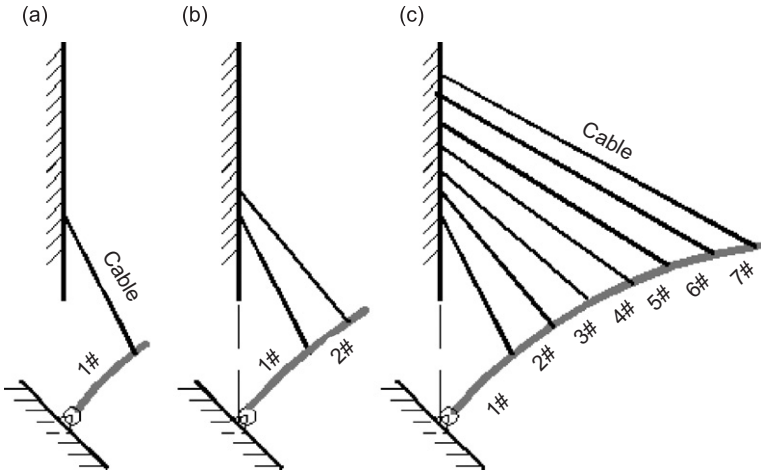


Fig. 11. Erection of arch of the (a) first segment, (b) second segment and (c) seventh segment.

Table 3
The lowest five frequencies of the erection of the arch (Hz)

| Mode no. | 1st | 2nd | 3rd | 4th | 5th | 6th | 7th | 8th |
|---|---|---|---|---|---|---|---|---|
| 1 | 11.199 | 11.491 | 9.9771 | 5.270 | 6.7765 | 4.9773 | 4.2273 | 5.2699 |
| 2 | 24.270 | 13.254 | 11.624 | 5.691 | 10.196 | 8.683 | 7.9531 | 5.691 |
| 3 | 70.217 | 31.132 | 18.141 | 8.535 | 13.592 | 12.101 | 11.284 | 8.535 |
| 4 | 112.40 | 61.748 | 35.034 | 9.048 | 18.567 | 14.949 | 13.987 | 9.0483 |
| 5 | 144.53 | 73.722 | 54.936 | 10.85 | 28.801 | 21.485 | 18.982 | 10.851 |

In the following section, a research on the frequencies of erection process of the arch bridge built using the cantilever construction method with tiebacks (Fig. 11) is investigated. The arch is divided to 15 segments, 1# to 7# belonging to the west main arch, and 9# to 15# belonging to the east and 8# connects both sides. The lowest five frequencies of the erection process of the arch are given in Table 3. While the segments increase, the frequencies of the arch decrease contrarily. In other words, the stiffness is reduced by an increase in the length of the arch with uniform cross-section

## 5. Conclusions

The term 'cable–arch structures' is commonly used in cable roofs and cable bridges; however, the dynamic model of cable–arch is proposed for the first time in this paper, and the governing equations of the cable–arch, considering the effects of axial extension and neglecting the effects of shear deformation and rotatory inertia, are derived according to Hamilton's principle for dynamic problems in elastic body under equilibrium state, in this paper. Then, by using the transfer matrix method and by neglecting the effects of axial extension, the exact solutions are obtained in terms of the boundary conditions (hinged–hinged, clamped–clamped and clamped–hinged, hinged-free). The same solution is employed for the cases in which the variable cross-sections of arch as well as the effects of parameters of cable and arch are considered. Compared to pure arch, obviously the cable–arch structure is more superior.

For all modes, the natural frequencies exhibit sharp increases for cable–arch with an increase in the stiffness, number and situation angle $\phi_1$ of the cable. On the contrary, the natural frequencies show clearly decreases in cable–arch with an increase in the opening angle $\varphi$ and the length of arch. However, the frequencies of

cable–arch are not sensitive to the boundary conditions: hinged–hinged, clamped–clamped and clamped–hinged. In other words, the cable can make a pure arch insensitive to boundary conditions. An important conclusion expounds that the natural frequencies of cable–arch are bigger than the pure arch but there is no significant change in the mode shapes.

In the literature, the discontinuity of arch has been considered for the pure arch and the cable–arch, and two kinds of step arches are investigated. The height and position of the cross-section of the arch affect the frequency.

The frequencies of erection process of the arch bridge are investigated. The frequencies of the arch decreases while the segments of the arch go on increasing.

The cases given in this paper are ultimately solved and the results are compared by finite element method. Between these results, absolute agreement can also be easily found. And all the cases show that cables improve the in-plane stiffness of the arch. The analysis results indicate that the program is accurate; meanwhile, the mechanical model and method are both valuable and significant not only in theoretical research and calculation but also in the design of engineering.

## Acknowledgments

This program is funded by the National Natural Science Foundation of China (70771038) and MDE Fund for Cross Century Talents (2002) 48. Interesting comments and criticism by the reviewers are also gratefully acknowledged.

## Appendix A

The elements of the matrix $\mathbf{T}$ in Eq. (27) are given as follows:

$$
\begin{aligned}
&T_{11}=\varphi, && T_{12}=\frac{1}{\beta}\mathrm{sh}\,\beta\varphi, && T_{13}=\frac{1}{\beta}\mathrm{ch}\,\beta\varphi,\\
&T_{14}=\frac{1}{\alpha}\sin\alpha\varphi, && T_{15}=-\frac{1}{\alpha}\cos\alpha\varphi, && T_{16}=1,\\
&T_{21}=1, && T_{22}=\mathrm{ch}\,\beta\varphi, && T_{23}=\mathrm{sh}\,\beta\varphi,\\
&T_{24}=\cos\alpha\varphi, && T_{25}=\sin\alpha\varphi, && T_{31}=\frac{\varphi}{R},\\
&T_{32}=\frac{1}{R}\left(\frac{1}{\beta}+\beta\right)\mathrm{sh}\,\beta\varphi, && T_{33}=\frac{1}{R}\left(\beta+\frac{1}{\beta}\right)\mathrm{ch}\,\beta\varphi, && T_{34}=\frac{1}{R}\left(\frac{1}{\alpha}-\alpha\right)\sin\alpha\varphi,\\
&T_{35}=\frac{1}{R}\left(\alpha-\frac{1}{\alpha}\right)\cos\alpha\varphi, && T_{36}=\frac{1}{R}, && T_{41}=-\frac{EJ_X}{R^2},\\
&T_{42}=-\frac{EJ_X}{R^2}(1+\beta^2)\mathrm{ch}\,\beta\varphi, && T_{43}=-\frac{EJ_X}{R^2}(1+\beta^2)\mathrm{sh}\,\beta\varphi, && T_{44}=-\frac{EJ_X}{R^2}(1-\alpha^2)\cos\alpha\varphi,\\
&T_{45}=-\frac{EJ_X}{R^2}(1-\alpha^2)\sin\alpha\varphi, && T_{52}=-\frac{EJ_X}{R^3}(\beta^3+\beta)\mathrm{sh}\,\beta\varphi, && T_{53}=-\frac{EJ_X}{R^3}(\beta+\beta^3)\mathrm{ch}\,\beta\varphi,\\
&T_{54}=-\frac{EJ_X}{R^3}(\alpha^3-\alpha)\sin\alpha\varphi, && T_{55}=-\frac{EJ_X}{R^3}(\alpha-\alpha^3)\cos\alpha\varphi, && T_{61}=-\frac{EJ_X}{R^3}x^2,\\
&T_{62}=\frac{EJ_X}{R^3}(\beta^4+\beta^2-x^2)\mathrm{ch}\,\beta\varphi, && T_{63}=\frac{EJ_X}{R^3}(\beta^4+\beta^2-x^2)\mathrm{sh}\,\beta\varphi, &&\\
&T_{64}=\frac{EJ_X}{R^3}(\alpha^4-\alpha^2-x^2)\cos\alpha\varphi, && T_{65}=\frac{EJ_X}{R^3}(\alpha^4-\alpha^2-x^2)\sin\alpha\varphi, && T_{77}=1,
\end{aligned}
$$

the rest elements of $\mathbf{T}$ are zero.

## Appendix B

The elements of matrix $\mathbf{T}_0^{-1}$ Eq. (30) are given as follows:

$$T_{12}=\frac{-x^2+(\alpha^2-1)(1+\beta^2)}{\alpha^2\beta^2},\quad T_{14}=\frac{R^2(\alpha^2-\beta^2-1)}{EJ_X\alpha^2\beta^2},\quad T_{16}=-\frac{R^3}{EJ_X\alpha^2\beta^2},$$

$$T_{22}=-\frac{1+x^2-\alpha^2}{\alpha^2\beta^2+\beta^4},\quad T_{24}=\frac{R^2(1-\alpha^2)}{EJ_X(\alpha^2\beta^2+\beta^4)},\quad T_{26}=\frac{R^3}{EJ_X(\alpha^2\beta^2+\beta^4)},$$

$$T_{31}=\frac{1-\alpha^2}{\alpha^2\beta+\beta^3},\quad T_{33}=\frac{R(\alpha^2-1)}{\beta(\alpha^2+\beta^2)},\quad T_{35}=-\frac{R^3}{EJ_X\beta(\alpha^2+\beta^2)},$$

$$T_{42}=\frac{1+x^2+\beta^2}{\alpha^2(\alpha^2+\beta^2)},\quad T_{44}=\frac{R^2(1-\alpha^2)}{EJ_X\beta^2(\alpha^2+\beta^2)},\quad T_{46}=\frac{R^3}{EJ_X\beta^2(\alpha^2+\beta^2)},$$

$$T_{51}=-\frac{1+\beta^2}{\alpha(\alpha^2+\beta^2)},\quad T_{53}=\frac{R(1+\beta^2)}{\alpha(\alpha^2+\beta^2)},\quad T_{55}=\frac{R^3}{EJ_X\alpha(\alpha^2+\beta^2)},$$

$$T_{61}=\frac{(1+\beta^2)(\alpha^2-1)}{\alpha^2\beta^2},\quad T_{63}=\frac{R(1+\beta^2-\alpha^2)}{\alpha^2\beta^2},\quad T_{65}=\frac{R^3}{EJ_X\alpha^2\beta^2},$$

$T_{77}=1$, the rest elements of $\mathbf{T}_0^{-1}$ are zero.

## References


[1] S. Markus, T. Nanasi, Vibration of curved beams, *The Shock and Vibration Digest* 13 (1981) 3–14.
[2] P.A.A. Laura, M.J. Maurizi, Recent research on vibrations of arch-type structures, *The Shock and Vibration Digest* 19 (1987) 6–9.
[3] P. Chidamparam, A.W. Leissa, Vibrations of a planar curved beams, rings and arches, *Applied Mechanics Reviews* 46 (1993) 467–483.
[4] N.M. Auciello, M.A. De Rosa, Free vibrations of circular arches: a review, *Journal of Sound and Vibration* 174 (1994) 433–458.
[5] Y.Y. Zhao, H.J. Kang, R. Feng, W.Q. Lao, Advances of research on curved beams, *Advances in Mechanics* 36 (2006) 170–186.
[6] P.A.A. Laura, P.L. Verniere De Irassar, R. Carnicer, R. Bertero, A note on vibrations of a circumferential arch with thickness varying in a discontinuous fashion, *Journal of Sound and Vibration* 120 (1988) 95–105.
[7] P. Chidamparam, A.W. Leissa, Influence of centerline extensibility on the in-plane free vibrations of loaded circular arches, *Journal of Sound and Vibration* 183 (1995) 779–795.
[8] M. Kawakami, T. Sakiyama, H. Matsuda, C. Morita, In-plane and out-of-plane free vibrations of curved beams with variable sections, *Journal of Sound and Vibration* 187 (1995) 381–401.
[9] G. Karami, P. Malekzadeh, In-plane free vibration analysis of circular arches with varying cross-sections using differential quadrature method, *Journal of Sound and Vibration* 274 (2004) 777–799.
[10] M.B. Rubin, E. Tufekci, Three-dimensional free vibrations of a circular arch using the theory of a Cosserat point, *Journal of Sound and Vibration* 286 (2005) 799–816.
[11] E. Tufekci, A. Arpaci, Exact solution of in-plane vibrations of circular arches with account taken of axial extension, transverse shear and rotatory inertia effects, *Journal of Sound and Vibration* 209 (1998) 845–856.
[12] E. Tufekci, O. Ozzdemirci, Exact solution of free in-plane vibration of a stepped circular arch, *Journal of Sound and Vibration* 295 (2006) 725–738.
[13] E. Tufekci, O.Y. Dogruer, Out-of-plane free vibration of a circular arch with uniform cross-section: Exact solution, *Journal of Sound and Vibration* 291 (2006) 525–538.
[14] P. Krishna, Tension roofs and bridges, *Journal of Constructional Steel Research* 57 (2001) 1123–1140.
[15] J.S. Ju, Y.L. Guo, In-plane elastic buckling of arch, *Tsinghua Science and Technology* 7 (2002) 322–325.
[16] X.Q. Cui, Y.L. Guo, H. Wang, Static behavior of pre-stress cable–truss hybrid structure, *Proceedings of the Sixth Pacific Conference on Steel Structures*, Beijing, October 2001.
[17] S.H. Hu, Y.L. Guo, The inelastic behavior of pre-stress cable–arch, *Advances Insteel Structures*, Shanghai, 2005.
[18] Y.Y. Zhao, J.G. Lu, Z.P. Yi, Study of mechanical behavior and economy of cable-stayed arch bridge, *Word Bridges* (2005) 29–32 (in Chinese).
[19] Y.Y. Zhao, X.Z. Yang, H.J. Kang, Analysis of dynamic characteristics for cable-stayed arch bridge, *Highway* (2005) 36–39 (in Chinese).
[20] Y.Y. Zhao, H.J. Kang, L.H. Wang, H.B. Zhou, Instability behavior in the plane of cable–arch structure, *Journal of Hunan University (Natural Sciences)* 33 (2006) 1–5 (in Chinese).
[21] T. Irie, G. Yamada, I. Takahashi, The steady state out-of-plane response of a Timoshenko curved beam with internal damping, *Journal of Sound and Vibration* 71 (1980) 145–156.

[22] T. Irie, G. Yamada, I. Takahashi, Natural frequencies of out-of-plane vibration of arcs, *Journal of Applied Mechanics* 49 (1982) 910–913.
[23] J. Henrych, *The Dynamics of Arches and Frames*, Elsevier Scientific Publishing Company, Amsterdam, Oxford, and New York, 1981.
[24] E. Viola, E. Artioli, M. Dilena, Analytical differential quadrature results for vibration analysis of damaged circular arches, *Journal of Sound and Vibration* 288 (2005) 887–906.
[25] K.B. Subrahmanyam, A.K. Garg, Uncoupled flexural vibrations of straight beams with all possible boundary conditions treated by a transfer matrix method, *Journal of Sound and Vibration* 204 (1997) 397–419.